Lawrence Berkeley National Laboratory

Title
MEMORY FILAMENTS IN AMORPHOUS As-Te-I SEMICONDUCTORS

Permalink
https://escholarship.org/uc/item/0mk236c2

Author
Roberts, Jon Allan

Publication Date
1974-12-01

MEMORY FILAMENTS IN AMORPHOUS As-Te-I SEMICONDUCTORS

Jon Allan Roberts
(M.S. thesis)

December, 1974

DISCLAIMER

.

MEMORY FILAMENTS IN AMORPHOUS As-Te-I SEMICONDUCTORS

Contents

MEMORY FILAMENTS IN AMORPHOUS As-Te-I SEMICONDUCTORS

Jon Allan Roberts
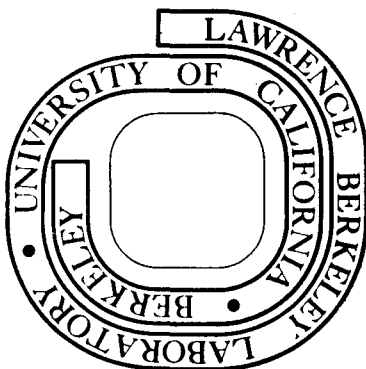
Inorganic Materials Research Division, Lawrence Berkeley Laboratory and
Department of Materials Science and Engineering, College of Engineering;
University of California, Berkeley, California

ABSTRACT

The memory effect in $As_{0.53}Te_{0.43}I_{0.04}$, an amorphous semiconductor, was studied by observing the memory filament optically, by electron microscopy and by electron beam microprobe. The filaments were found to be crystalline tellurium, formed by diffusion activated by joule heating and under the influence of the applied electic field. Several growth morphologies were observed, but the general formation pattern included initiation at the positivily charged probe and a growth rate toward the negative probe which was independent of applied current level and pulse duration. The electron microscopy of extracted filaments showed the filaments were often single crystals, although produced by pulsed current application, and there is some evidence of a preferred crystallographic orientation for the filaments. The electron beam microprobe studies showed the diffusion of tellurium to the growing end of the filament is primarily radial, although near 100% completion, the axial depletion is more severe, and the high negative resistance of the small remaining gap often prevents successful completion of the filaments under this diffusion mechanism.

I. INTRODUCTION

Several compositions of chalcogenide glasses have been shown to demonstrate a memory effect in addition to a switching phenomenon.[1,2,3] In the switching effect, the voltage applied across a sample of the bulk material can be increased to a maximum value, V_{TH}, with a high value of resistance, at which point the material switches to a low resistance state. When the applied power is removed, the material reverts to its high resistance state. In compositions with the memory effect, switching, followed by the application of a critical current level establishes a second phase in the glass confined to a narrow filamentary path which has been associated with the filamentary current path established in materials with the same current-controlled negative differential resistance.[4] After removal of the applied power, the material in the filamentary path remains in a low resistance state. A short application of a current higher than the above critical current results in the destruction of the path, probably by melting, and the re-establishment of the high-resistance state on quenching the path after the end of the current pulse.

The composition selected for this study is $As_{0.53}Te_{0.43}I_{0.04}$, reported by Pearson[5] to display the memory effect. The solid solubility of As in Te is given as 0.005 at.%,[6] and a metastable solid solution produced by quenching an homogeneous liquid solution would separate into pure As and Te phases, given sufficient mobility of the components. Since As is the higher melting component, a filamentary path formed by joule heating during power application should be composed of As crystallites, surrounded by a crystalline Te phase. Further, the joule heating should

be uniform, at least for small devices, over the entire switching volume, and such a transformation should occur approximately simultaneously over this volume.

The experiments of Pearson used a bulk geometry, with contacts placed on opposite sides of a thin specimen. Such an arrangement prevents direct observation of the transformation. The work of Utteoht,[7] et al., placed the electrical contacts on the same side of the specimen, in a planar geometry. They observed a polarity dependence of the transformation in their material, $As_{0.55}Te_{0.35}Ge_{0.10}$. The transformation occurred initially at the positive probe contact, and extended to join the negative probe to establish the memory state. Further, their results indicated the filament is enriched in tellurium. These two observations indicate the mechanism of the transformation is other than that of thermal decomposition.

II. SAMPLE PREPARATION

A. Alloy Preparation

The components were weighed under a nitrogen atmosphere and placed in a cylindrical quartz capsule measuring 2 cm in diameter and 10 cm in length. The capsule was cooled in liquid nitrogen to reduce the vapor pressure of the components, particularly iodine, and evacuated to 10^{-3} torr before sealing. The capsule was then placed in a molybdenum cylinder to protect against possible explosion, and heated in a horizontal tube furnace to 1000°C. The melt was held at this temperature for three days, cooled to 500°C in the furnace, and then water quenched, still within the molybdenum cylinder.

The resulting ingot had a density of 3.81 $g\text{-}cm^{-3}$ and was severely cracked by the thermal shock of the quench. Analysis with the electron beam microprobe showed composition variations of less than 5% over distances of about 2 micron, although no evidence of phase separation could be found optically. A second melt was prepared using an oil quench; here the cracking was less severe, but regions of about 1 mm in extent were found to have separated into arsenic and tellurium crystallites. Samples used in this study came exclusively from the water-quenched melt.

B. Metallographic Preparation

Small chunks, about 1 cm in extent, were broken off the ingot and coated in low melting point wax to prevent cracking under mounting stresses. The samples were then mounted in room temperature setting resin. A plane surface was then ground and polished. The final polishing treatment used 0.05 micron alumina suspended in water.

III. EXPERIMENTAL APPARATUS

A. Contacts

Electrical contact with the specimen surface was made with two pointed tungsten probes. The probes were prepared by electropolishing to a probe diameter of about 1μ. One probe was fixed on the optical axis of a microscope, while the other was mounted on an X-Y translatable stage. Both probes could be translated simultaneously in the vertical direction. The sample was mounted on a second translatable stage and raised to the microscope focal plane. After selecting the desired viewing area, the probes were lowered to the sample surface, and the position of the translatable probe adjusted for the desired spacing and orientation. Thus, parallel rows of filaments using nearly identical spacings could be formed by translation of the specimen. The probe pressure was kept approximately constant from one region to another by measuring the vertical displacement of the probes with respect to the focal point of the microscope, and by keeping the specimen surface in focus. The probe positioning and filament growth were observed at about 250× magnification.

B. Power Application

The electric current was applied in pulses, using a voltage pulse generator driving a transistor as a current source, with emitter resistor feedback. This arrangement is shown in Fig. 1. The circuit was designed to develop current pulses from 0.1 to 10 mA peak current level, rise and fall times from less than 1 msec to more than 1 second, and similar hold times. The pulse repetition rate was generally held
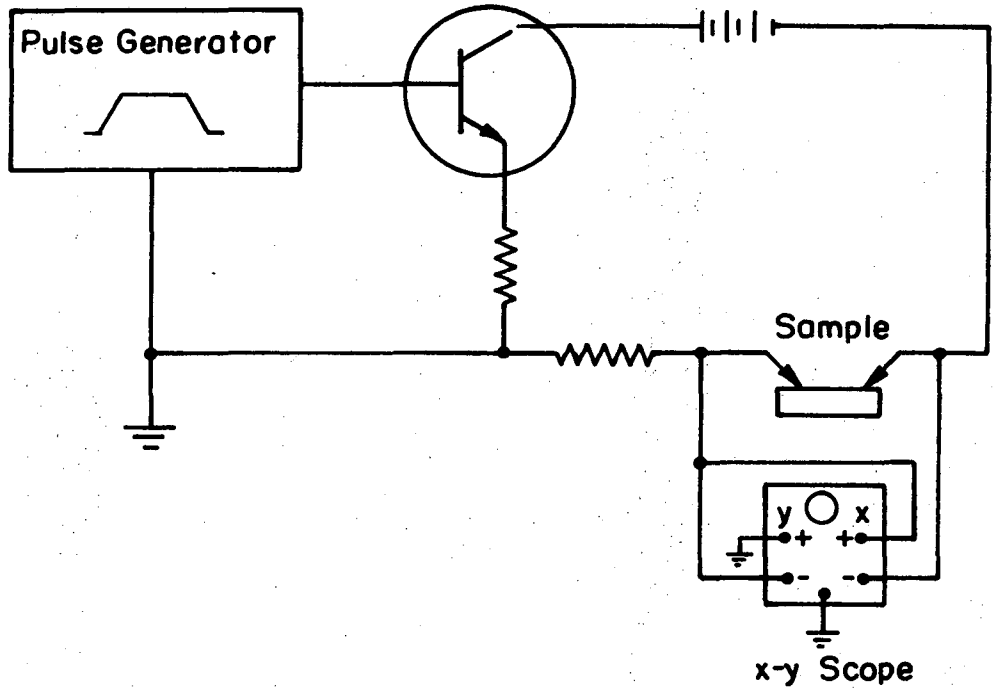
XBL732-5808

Fig. 1. Schematic of the current source apparatus used for
power application.

to 1 sec^{-1}. This method is believed superior to the use of a voltage pulse driving the device and a series limiting resistor because of the ability of the former to control capacitive charging of the material and to allow for the changing resistance of the load during formation. Pulsed power applications is preferred to continuous application so that growth rate studies may be performed.

IV. SWITCHING OBSERVATIONS

A. Constant Energy Condition

The external driving circuit used in this work was a current source. Therefore, the I-V curve traced out during switching resembled that of Pearson.[5] However, the shape of the curve was found to be strongly affected by the shape of the trapezoidal current pulse, i.e., the rise time of the pulse. Figure 2 shows two extremes of this effect. A relation was found between the rise time, t_r, and the threshold voltage, V_{TH}, at which switching occurs:

$$V_{TH} = k_1 t_r^{-k_2}$$

To show that the switching occurs as a result of total energy input, we integrate the power dissipated into the device prior to switching, assuming the I-V curve to be linear over $0 \leqslant V \leqslant V_{TH}$, and find the energy input for a single pulse

$$E = \frac{k_1^3 t_r^{1-3k_2}}{3R^2 I_{max}}$$

where R is the slope of the I-V trace, and I_{max} is the peak pulse current. From Fig. 3, we find for $I_{max} = 1.0$ mA,
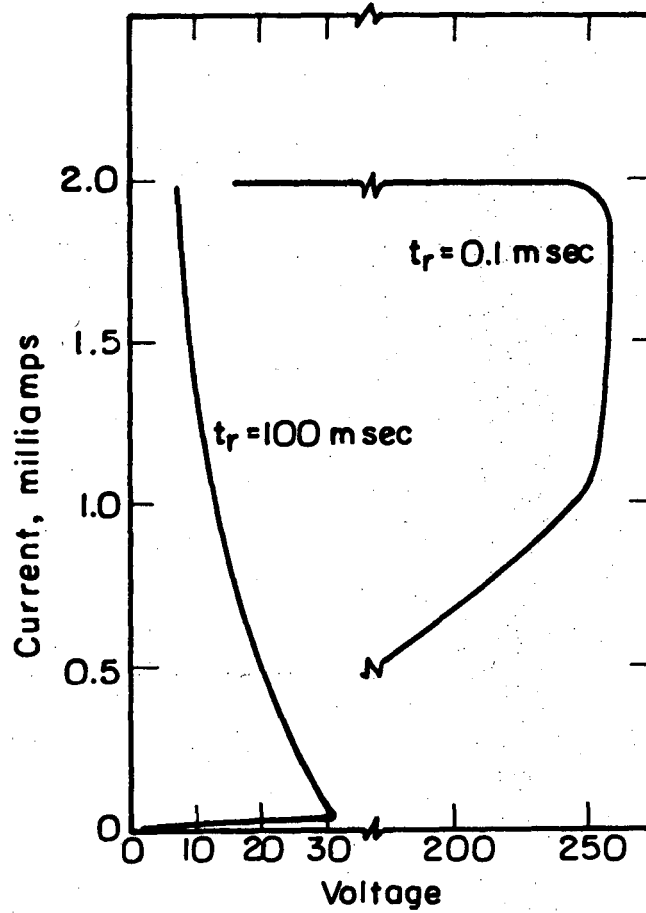
$$k_1 = 112$$

$$k_2 = 0.339$$

using units of volts and milliseconds; for R = 250,000 ohms the energy for switching is seen to be constant,

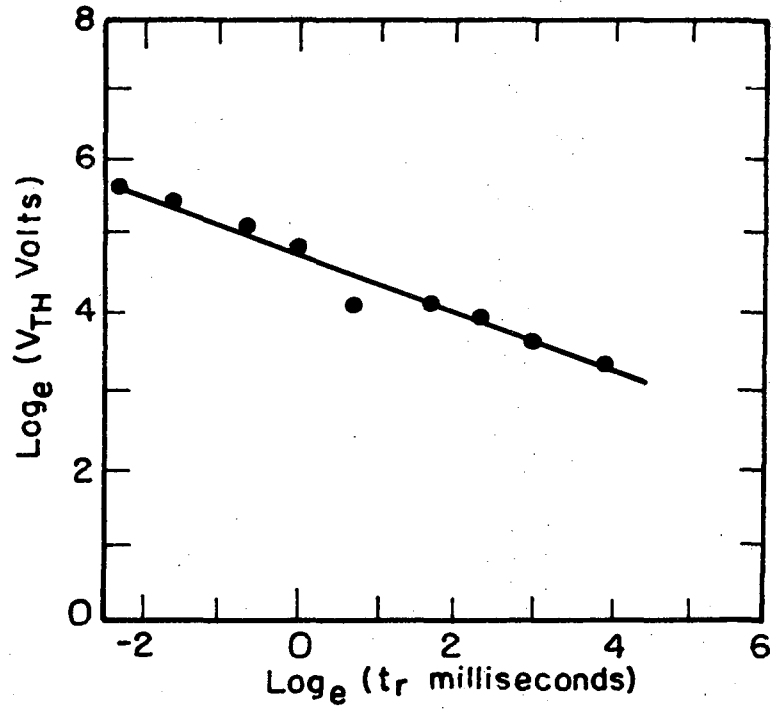$$= 3.7 \times 10^{-6} \text{ joules}$$

for a probe spacing of 150 microns.

Fig. 2. The effect of current pulse rise time on the
I-V characteristic.

XBL732-5810

Fig. 3.   Threshold voltage, V_{TH}, as a function of the
current pulse rise time.

To estimate the heating effect of this energy added adiabatically to the region between the probes during the pulse rise time, we take 0.06 cal/gram to be an estimate of the specific heat of the alloy. The region of material affected by switching (see Fig. 4) appears to be about 15 microns wide. With the density of the glass of 3.8 grams cm^{-3}, we have a temperature increase of about 300°C which is sufficient to soften the glass considerably.

B. Surface Distortion

The surface distortion seen prior to the growth of memory filaments occurs during the first few switching pulses. Figure 4 shows a cross-section taken about midway between the probes. Because of this shape, the distorted region is called the hillock. During the applied current pulse, the energy dissipated at the peak current level is of the order of 2×10^{-4} joules for a typical pulse length of 10 milliseconds, sufficient by the above calculations to rise the temperature of the hillock by 10^4°C; assuming the density is unchanged by the switching cycle, the hillock may be formed by thermal expansion. The constraint of the unsoftened matrix material induces plastic flow in the softer axial region of the hillock as the periferal material cools after termination of the pulse.
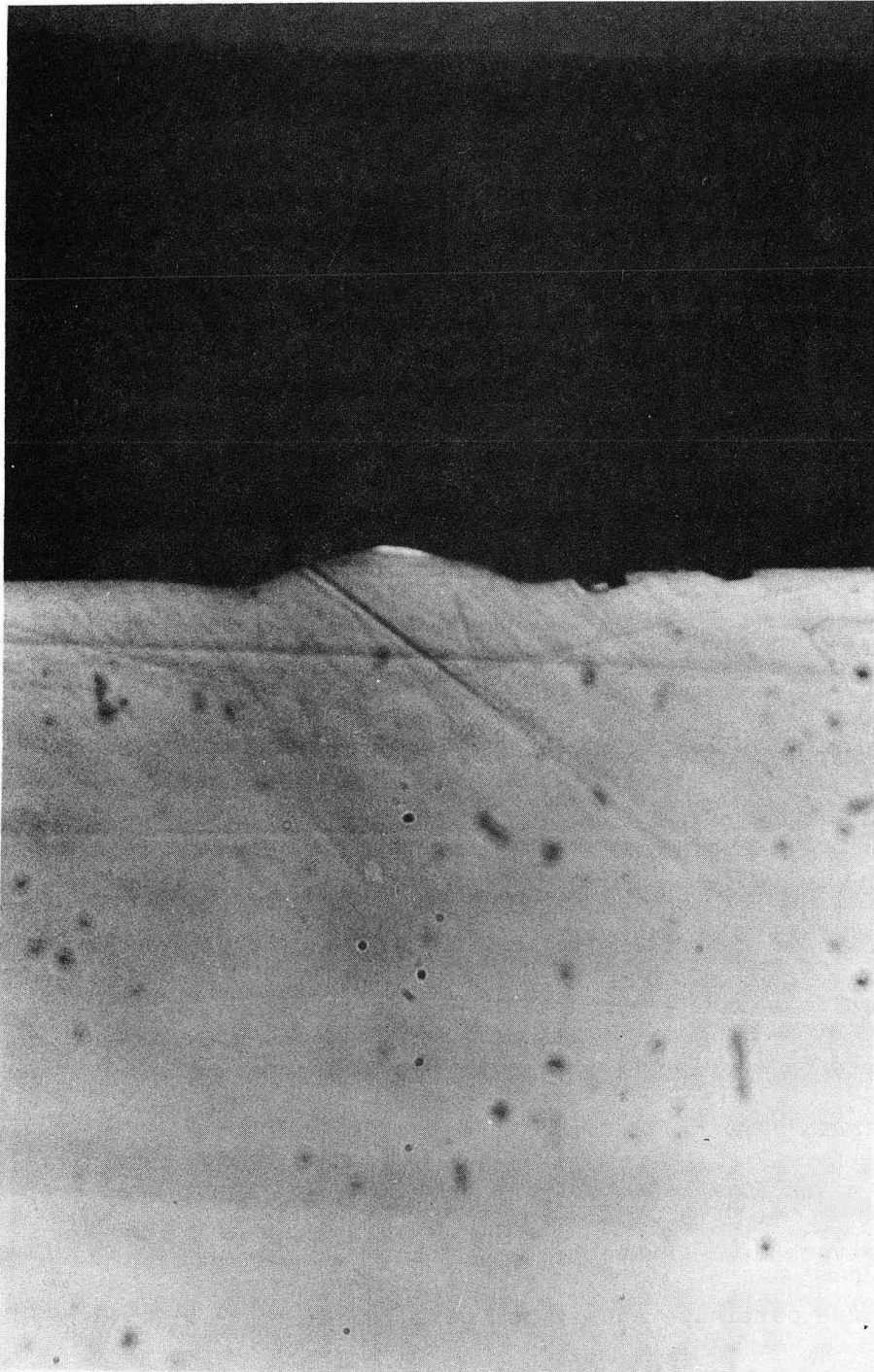
XBB 732-1103

Fig. 4. Cross-section of typical hillock and filament,
taken perpendicular to the axis and midway
between the probe contacts. The thin white
layer is the filament, seen to be about 3 microns
thick, 2000×, unetched.

V. FILAMENT GROWTH OBSERVATIONS

A. Physical

Generally, many of the filament growth observations parallel those of Uttecht, et al.,[7] in that the filament nucleates at the positive probe and grows in a more or less straight line toward and finally joins the negative probe. When this growth is complete, the I-V characteristic becomes fairly linear, with a resistance of about 5000 ohms. Although the growing filament is generally confined to the hillock, occasionally the filament may grow out of the initial hillock, in which cases, the distorted area is widened to include the errant filament during growth. A typical completed filament is shown in Fig. 5.

Two types of filament are found to grow from the positive probe: surface and subsurface. The surface filaments are generally segmented, due to the pulsed power application, while little evidence of segmenting is found in the subsurface growth. The surface filaments are often curved, while subsurface filaments are generally very straight. The growth rate of surface filaments is much faster than that of the sub-surface ones. Typical examples of these "normal" growth types are shown in Figs. 6 and 7.

Two types of negative probe growth are observed: small blocky second phase particles appear and grow in length toward the positive probe only a short distance. This growth appears in Fig. 8. During their formation, positive probe growth is halted. The second type, shown in Fig. 9, is subsurface, straight, and often grows faster than the positive probe growth. Both types are conductive as evidenced by the absence of an electrical breakdown when they are met by positive
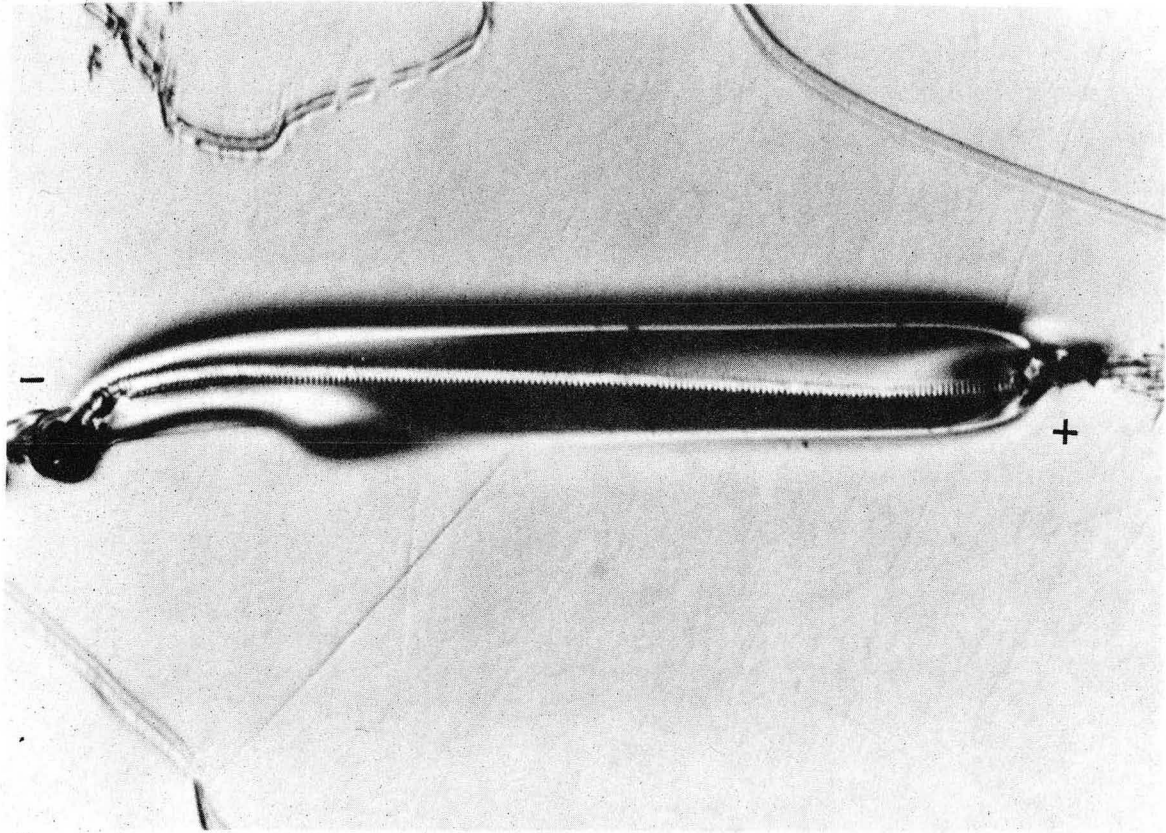
XBB 736-3683

Fig. 5. A typical completed filament formed by pulsed current application
1000×
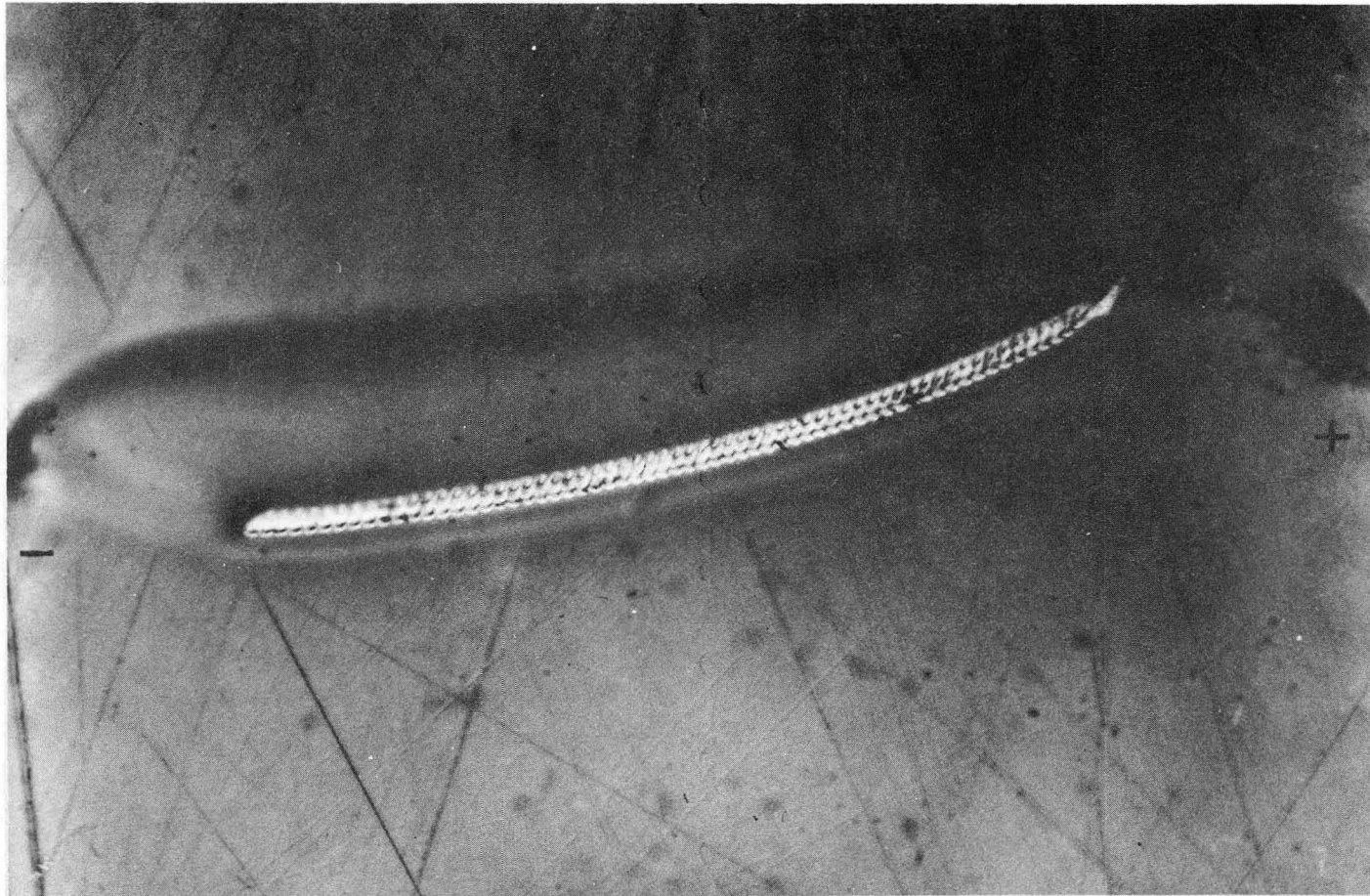
XBB 732-1164

Fig. 6. A partial surface filament, showing initial subsurface growth, and a second nucleation event beginning the surface growth, 1000×, unetched.
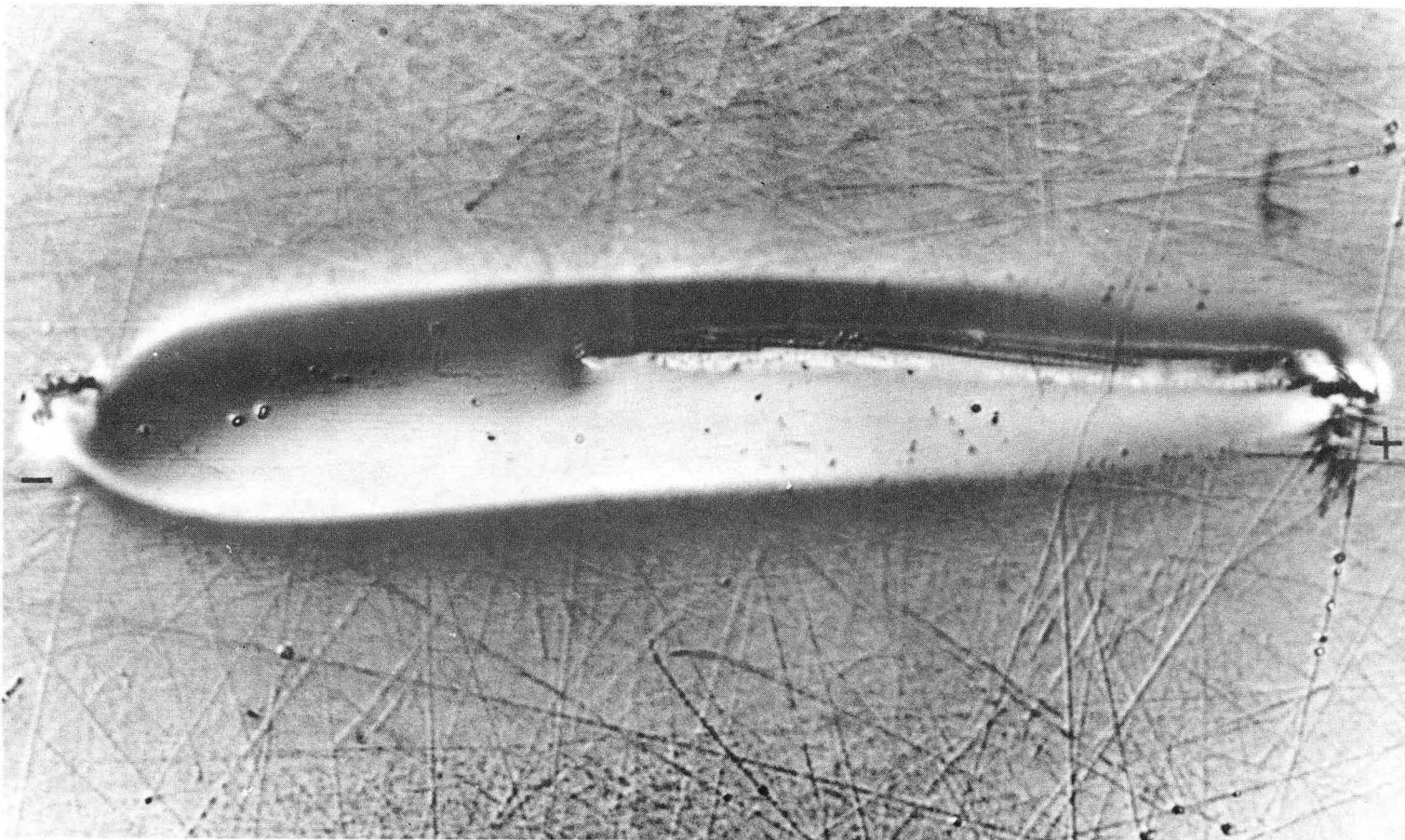
XBB 732-1165

Fig. 7. A partial subsurface filament. Note the poorly defined segmenting and longitudinal striations within the filament which may be boundaries of columner grains 1000×, unetched.

XBB 732-1166

Fig. 8.   A filament with initial and final subsurface growth, showing blocky second
phase growth at the negative probe 1000×, unetched.

XBB 732-1167
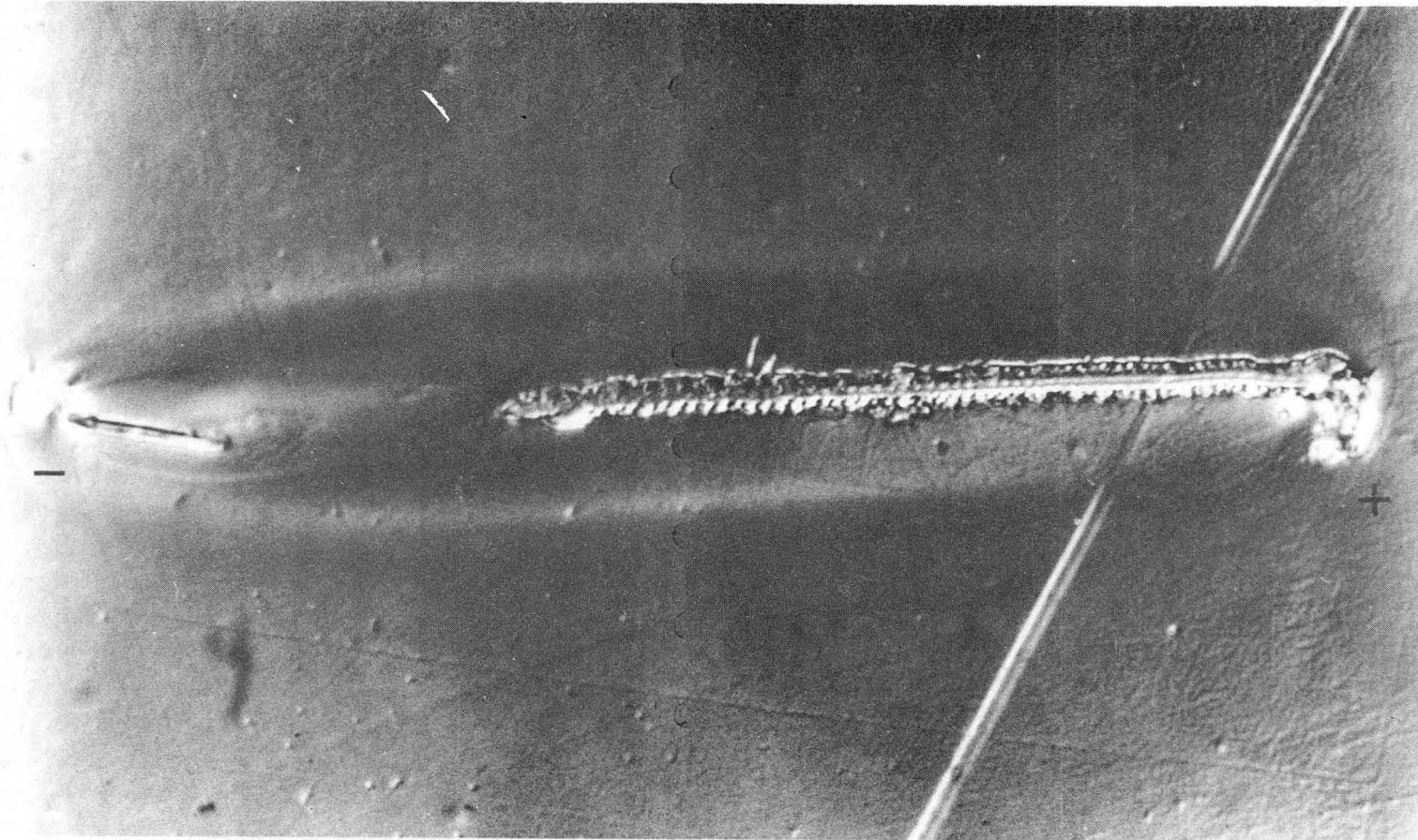
Fig. 9. A subsurface filament, with subsurface negative probe growth revealed by etching 1000×.

probe filament.

In addition to these, there are other types of phase separation. Nucleating at the positive probe, and occasionally nucleating at the end of a normally growing filament, a "leaf" shaped filament can grow, being much wider and advancing much slower than the other types. This structure often develops holes in the growing end, which change shape and position with each pulse. An example of the "leaf structure" is given in Fig. 10. Finally, nucleation of new phases can occur along the entire length of the probe spacing, forming many small crystallites which finally join to make a conductive path.

These several morphologies of phase transformations point out the prime difficulty in studying the memory state. Placing a particular growth in one of the above categories is sometimes ambiguous. The choice of which category a given growth will take is somewhat random, although the electrical parameters have some effect on the probabilities of the selection. Probably a more important effect is that of com-position variations in the matrix.

In order to narrow the study to a manageable size, the surface growth has been selected for further investigation. The segmented surface provides a measure of growth progress. The alignment of the segment "ribs" is generally normal to a line taken from the segment to the negative probe, especially notable in the case of curved surface filements. This observation indicates that the rib formation occurs during the electrical breakdown at the beginning of each pulse. Growth of the segment, however, is strongly influenced by the orientation. The preferred growth direction of the filament, shown later in this

XBB 732-1161

Fig. 10. A subsurface filament which has changed to the "leaf" structure during growth
1000×, unetched.

report to be crystalline, is usually not parallel to the flux of that
component making the filament, since the orientation of the initial segment
is probably random. The growth of a segment with respect to the initial
hillock axis would then depend on the extent of this misalignment.

B. I-V Curve Changes During Formation

Three important features of the I-V curve were tracked during formation
of a filament and are shown in Fig. 11: maximum voltage (V_{TH}), on-state
voltage (V_{ON}), and negative resistance (slope of I-V curve at the inflec-
tion point). Both the on-state voltage and the threshold voltage
decrease fairly linearly as the switched region becomes shorter, but the
negative resistance indicates a much faster increase. This effect may
be due to changes in hillock composition. The last few microns of
growth are often accompanied by severe oscillations of both voltage
and current, which occasionally result in distruction of the previously
grown filament. The oscillation is probably due to the frequency
response of the current source and the high negative resistance of the
small amount of hillock remaining near 100% completion.
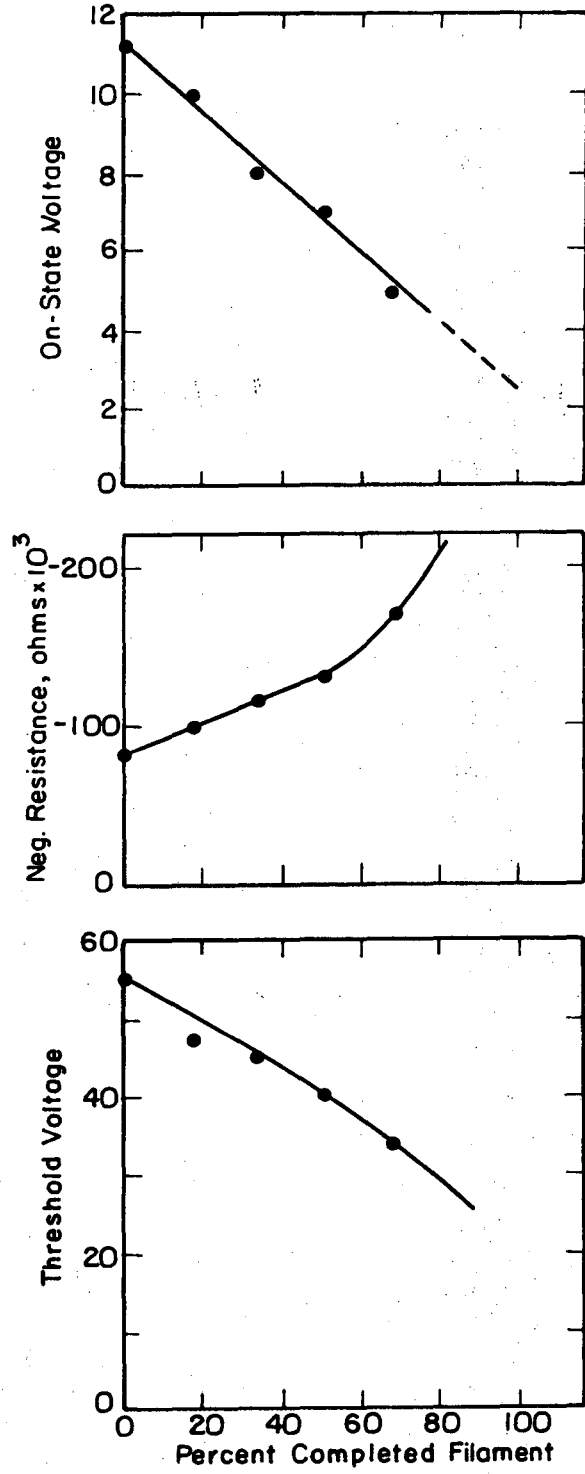
XBL732-5811

Fig. 11. Changes in parameters of the I-V curve during
growth of the filament.

VI.   ELECTRON MICROSCOPY OF FILAMENTS

The small size of the conductive paths make their identification by
X-ray diffraction unattractive. As shown in the cross sections of
Fig. 4, the filaments appear to be thin enough for electron microscopy
if removed from the matrix. A two-stage extraction replica technique
was developed to provide specimens for this effort. About 20 filaments
were formed over an area about equal to that covered by a microscope
grid and etched for 60-90 minutes in a mixture of 15 ml CS_2 and 240 ml
CH_3OH to which 0.5 ml Br_2 were added just before use. When the surface
had been sufficiently attacked, optical examination showed the filaments
to be standing 3-4 microns above the surface of the etched hillock. The
filaments are then extracted on a slice of plastic replicating film
(104-A, 0.0034 mm thick, Ted Pella Co., Tustin, CA) which has been
softened with a small drop of methyl acetate. Usually the extracted
filaments contained a few adherent particles of the matris. If the
etching time had been ideal, the filaments were attached to the matrix
along a small portion of their lengths, and these small particles
presented no difficulty in transmission. If the etching was carried too
far, the filaments became detached from the matrix and were quickly
attacked by the etchant. Replicas with large pieces of matrix adhering
to the filament could be cleaned by sandwiching the plastic film between
glass slides, and under microscopic examination, administering a few
drops of the diluted etchant to the replica. Some thinning of the
filaments occurred during this step. The cleaned replica was then coated
with evaporated carbon, and the plastic removed by dissolution in methyl
acetate. The carbon film was protected during dissolution by a smear of

petroleum jelly, which in turn was removed by soaking in CCl_4.[8] The

carbon film was then washed in alchol and water and retrieved on a

microscope grid. Typically, two or three filaments were found to be

suitable for examination from each group of twenty. The remainder were

lost during extraction, cleaning and dissolution steps. Filaments

prepared in this way were rarely good TEM specimens. They were typically

warped, often torn, and had been attached to an uncertain degree by the

etchant.

Figure 12 shows an extracted surface filament. Diffraction patterns

are shown for each of four successive segments in the growth direction.

As the electron beam microprobe results to be discussed later indicate,

the filament may be assumed to be tellurium, and these diffraction

patterns so indexed give d-spacings and interplanar angles consistent

with tellurium. The surface of the filament nearly coincides with the

(121) plane, and the growth direction is nearly parallel with the [$\bar{1}$01]

direction.

Figure 13 is an extracted subsurface filament; only the tip of this

specimen is thin enough for transmission, but its orientation is found

to be the same as in Fig. 12. This specimen had been attacked during

cleaning.
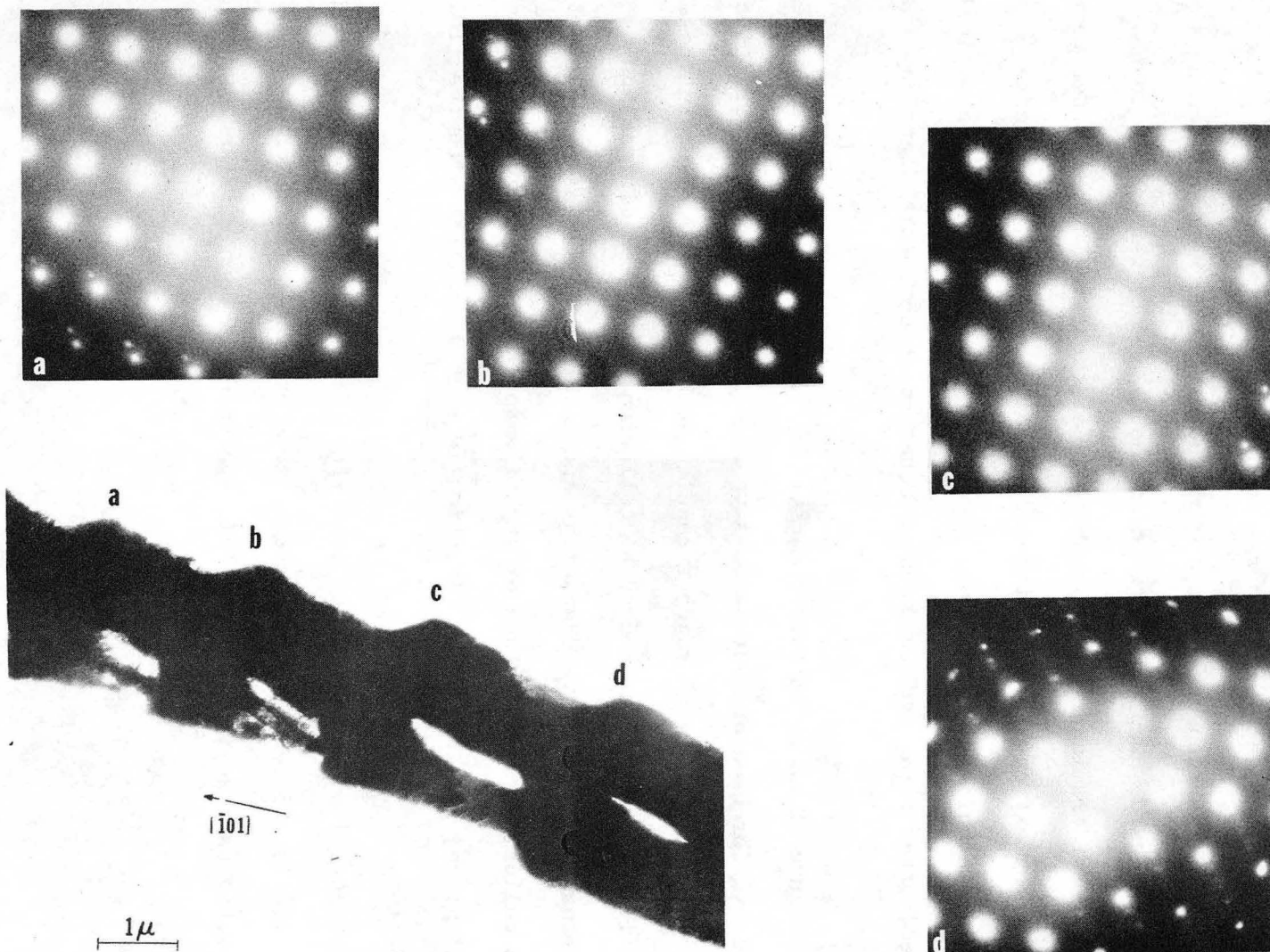
XBB 732-1160

Fig. 12. Electron diffraction patterns of four successive segments of a surface filament. The growth direction is to the left, approximately parallel to the {$\bar{1}$01} direction. Note the lack of rotations in the patterns of successive segments, indicating the growth of the filament as a single crystal. Holes shown in the filament image are due to tearing during extraction 650 kV Hitachi Electron Microscope.
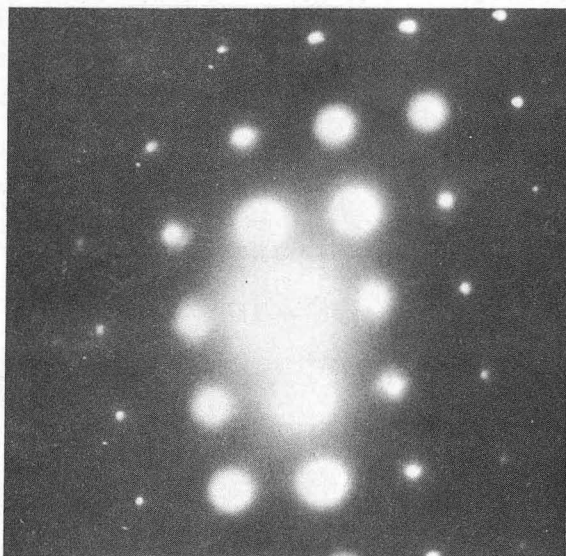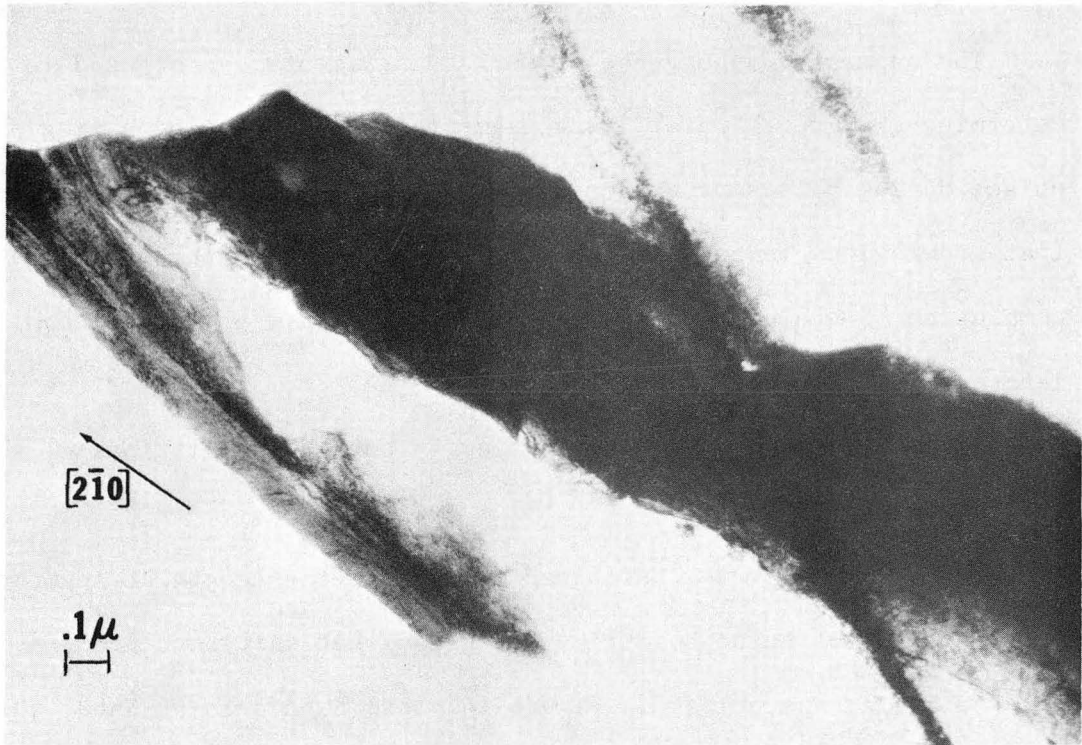
Fig. 13. An extracted subsurface filament growing in the [2$\bar{1}$0] direction 650 kV Hitachi Electron Microscope.

VII. GROWTH RATE STUDY

The segmented appearance of surface filaments can be used to determine the growth rate. Each segment is formed during a single pulse; during pulses of extremely long duration (1 sec), it was verified that growth does indeed occur during a pulse and terminates at the completion of the pulse. In general, the segments are of uniform length along the hillock, although growth near completion at the negative probe is often slower, and accompanied by severe oscillations of voltage and current.

Two experiments were performed to measure the length of segment as a function of pulse hold time using somewhat different probe spacings for the two groups of data. Figure 14 plots both sets of data, showing an approximately linear dependence. Since the pulse has the shape of a trapezoid, some growth occurs during the rise and fall times of the pulse, and therefore the plot shows an intercept of 0.5μ. The scatter is seen to be more severe for longer pulse durations. Since the thermal decomposition exists as an alternative phase transformation mechanism it can be expected that longer pulse durations produce sufficient heating to activate it. Secondary growth, as shown in Fig. 15, due to heating effects, compete with the primary growth by depleting the diffusion source.

A third experiment was performed to determine the effect of the peak current on the growth rate. Here, the rise and fall times, and pulse duration were held constant for a series of nearly identical probe spacings. As shown in Fig. 16, the correlation is negligible, and it can be concluded that the peak current, and therefore, the
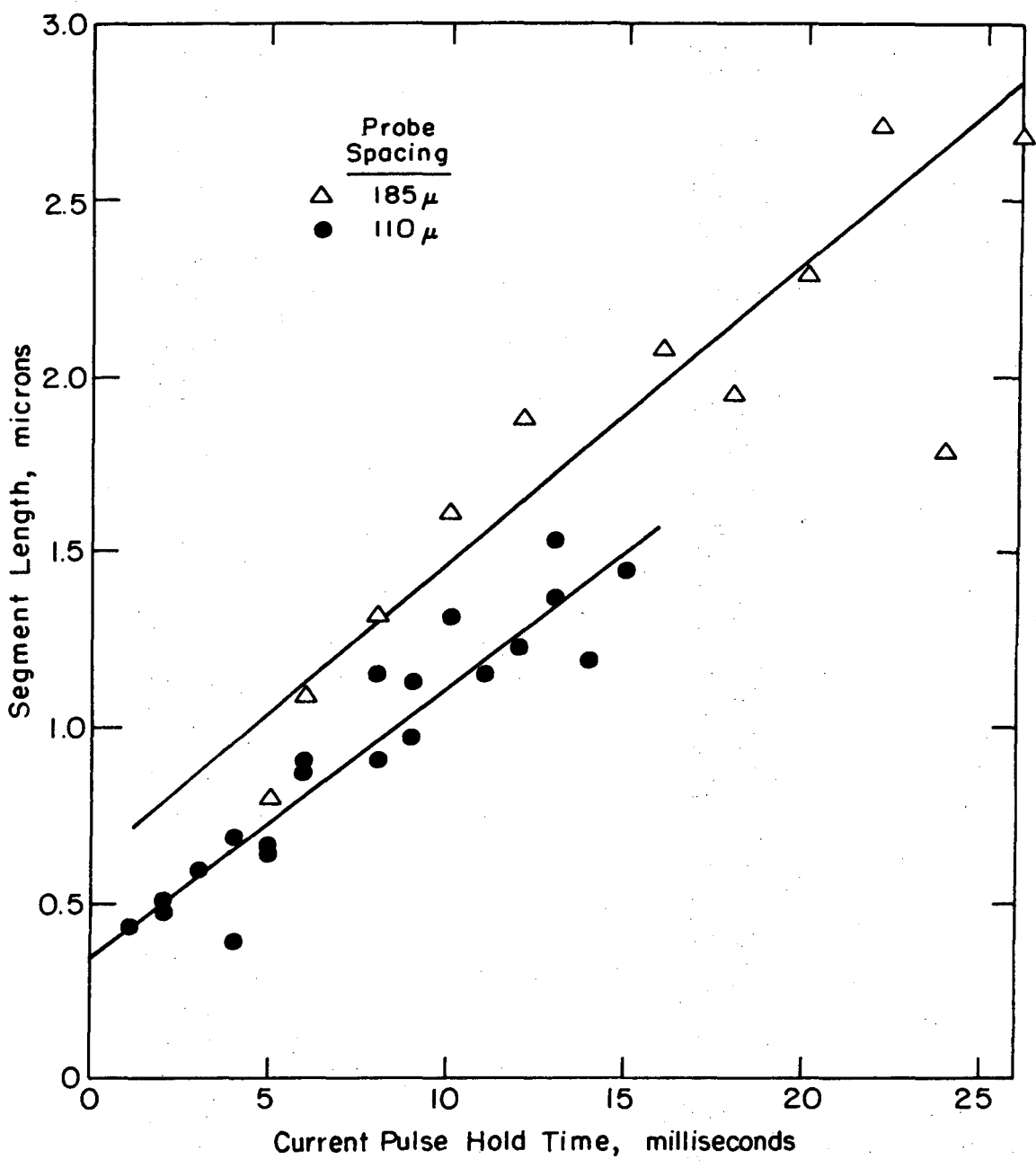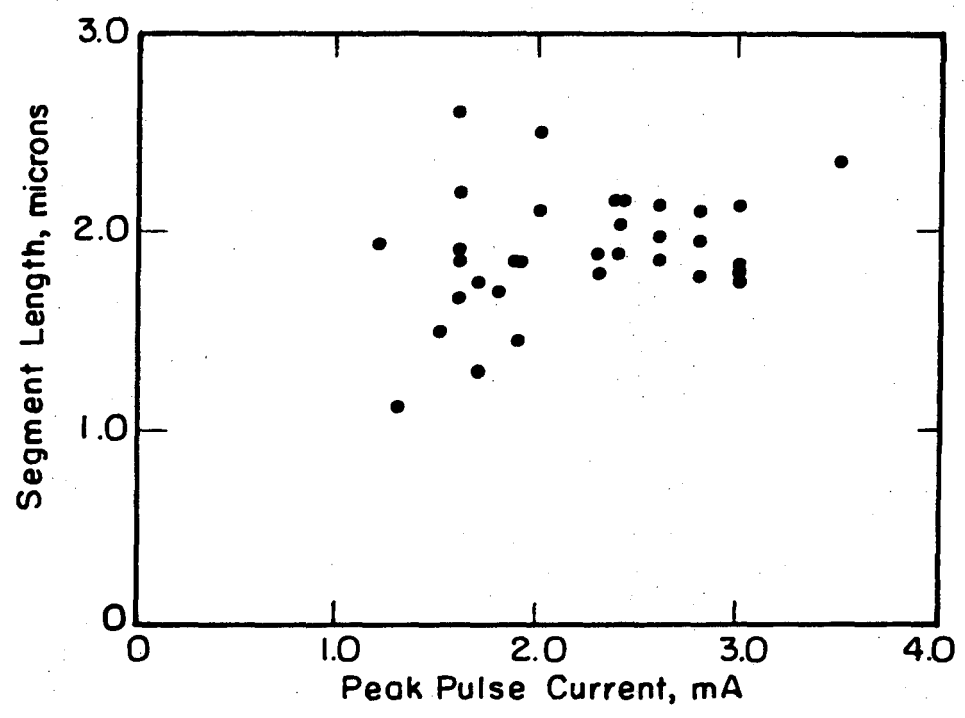
Fig. 14. Growth of surface filaments as a function of the current
pulse hold time.
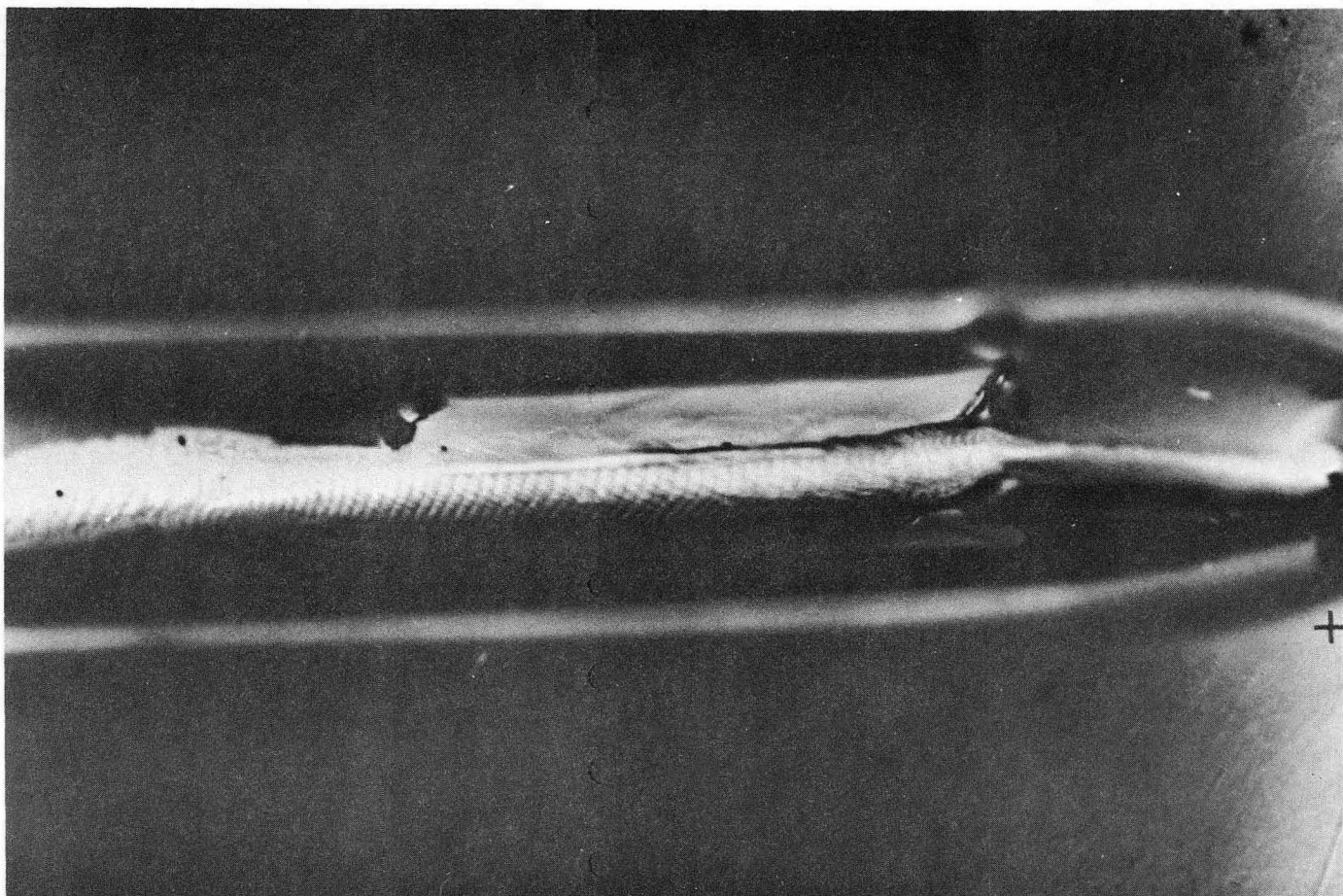
XBL732-5812

XBB 732-1162

Fig. 15. Secondary growth adjacent to a surface filament, occurring as a result of
heating during pulsing at a duty cycle of 5% 1000×, unetched.

XBL732-5813

Fig. 16. Poor correlation between growth rate of surface
filaments and the peak current level.

the heating effect of the power dissipation, is not directly responsible

for the phase separation.

VIII.   ELECTRON BEAM MICROPROBE STUDIES

A.   Experimental Problems

Extensive studies of concentration changes occurring before and during filament growth were undertaken, but a variety of factors limit their quantitative validity.   Since the glassy matrix is a poor electrical conductor, the surface of all samples were coated with a layer of evaporated carbon.   The electron beam evaporates some of the carbon, leaving a track by which the position of the beam is known; however, loss of the carbon conductor permits charging of the sample and therefore the beam wanders somewhat during each counting period.   Since the glass is a poor conductor, the beam heats the sample, and in regions of concentration gradients, thermally assisted diffusion can affect the accuracy of the X-ray counts.   The X-rays are excited in a volume of 3-5 cubic microns, and therefore averaging of the composition occurs. Finally, surface distortion affects the take-off angle from sample to detector; for these reasons, the microprobe data is reported as counts per second per unit beam current, and can be considered only qualitatively significant.

B.   Composition of the Filament

In Fig. 17, the results of a microprobe traverse normal to a filament shown that the filament is enriched in tellurium.   It is notable that the regions adjacent to the filament do not appear to be depleted in tellurium concentration, although a large and only slightly depleted zone might escape detection.
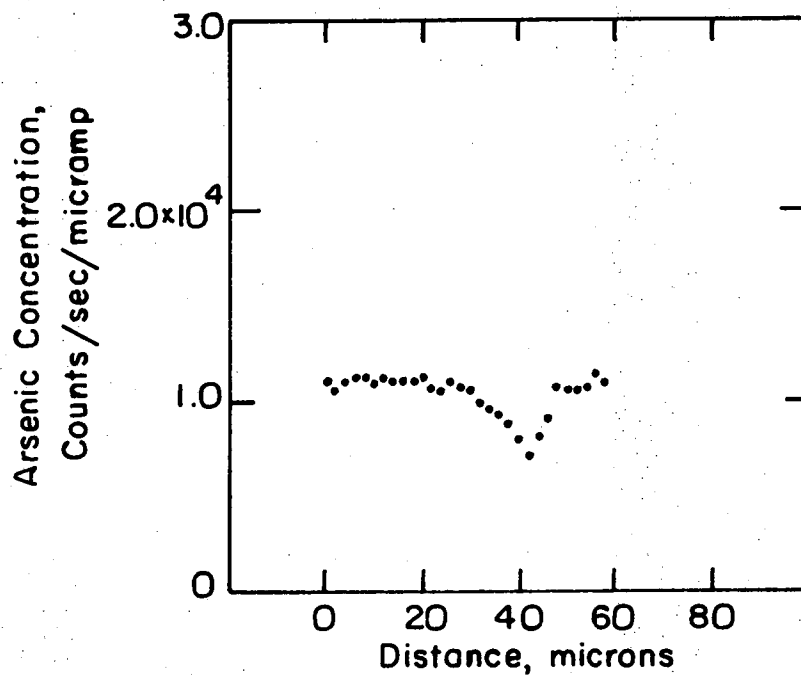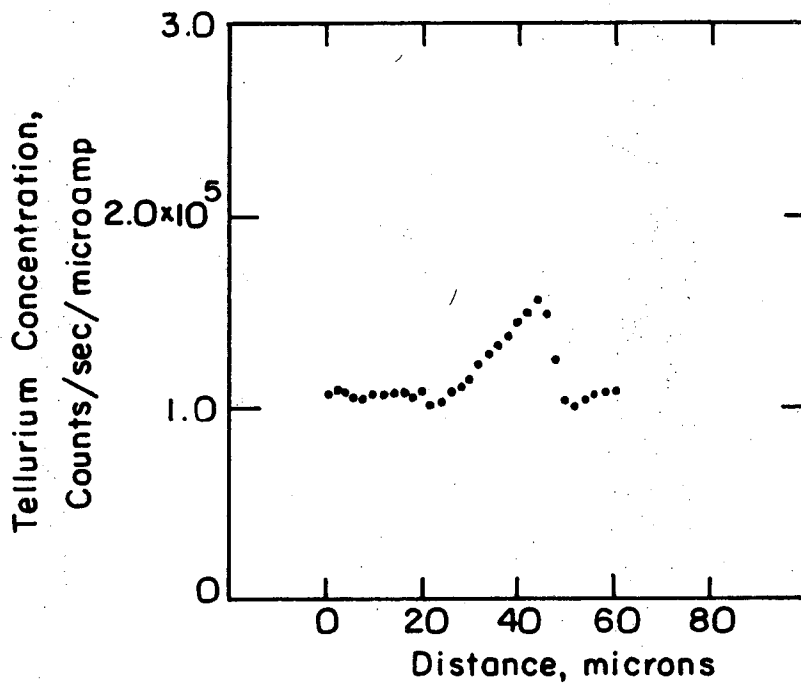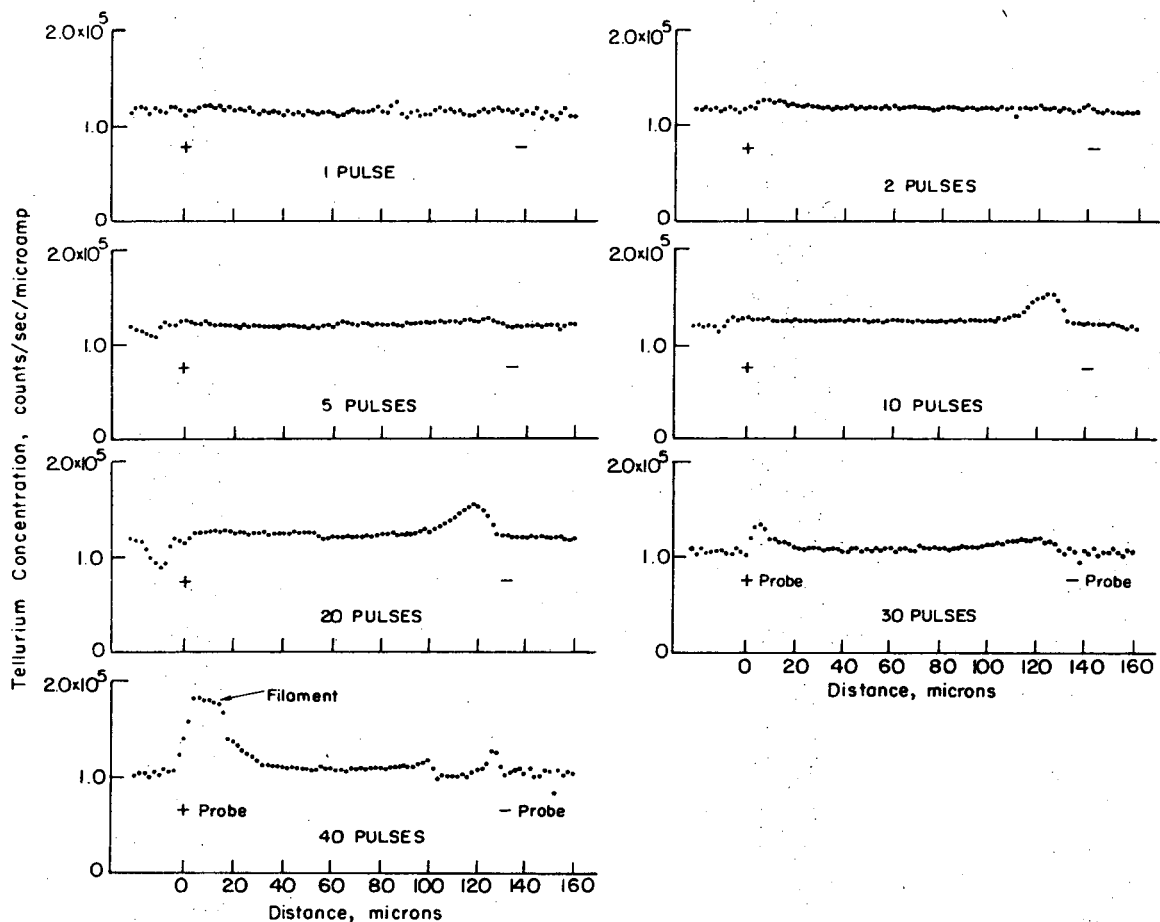
XBL 732-5814

Fig. 17. Arsenic and tellurium concentrations across a surface
filament.

C. Accumulation of Tellurium Prior to Nucleation

The results of an experiment consisting of a series of hillocks to which an increasing number of pulses were applied is shown in Fig. 18. Here the microprobe traverse was taken along the axis of the hillock. Although it is possible that slight shifts of the probes between successive pulses prevented nucleation on the first pulse, it appears that significant accumulation of tellurium does not occur until about 30 pulses, of about 7 milliseconds duration each.

Of special note in these plots is the smoothing of the scatter in tellurium concentration in the hillock region, when compared to the matrix. It suggests that during the alloy preparation, some phase separation did occur. If during the hillock formation (first few switching cycles) some degree of heating occurred, this region of the alloy would be "remelted" and quenched at a more rapid rate than the initial ingot cooling, thus making a more homogeneous composition. Accumulation of tellurium at the negative probe occurs during the first few pulses, and occasionally remains even during growth of the normal filament. This accumulation can result in the precipitation of a small crystalite of tellurium, as discussed previously.

An attempt was made to define the position on the I-V curve at which tellurium accumulation began. Ten pulses were applied to each of six hillocks, increasing the peak current for each and recording the I-V curve for those pulses. The I-V curves are shown in Fig. 19. The axial traverses of Fig. 20 shows that negative-probe accumulation of tellurium occurs at a level of 400 μA, but positive-probe accumulation not until a level between 0.6 mA and 1 mA peak current. Thus, the two accumulations
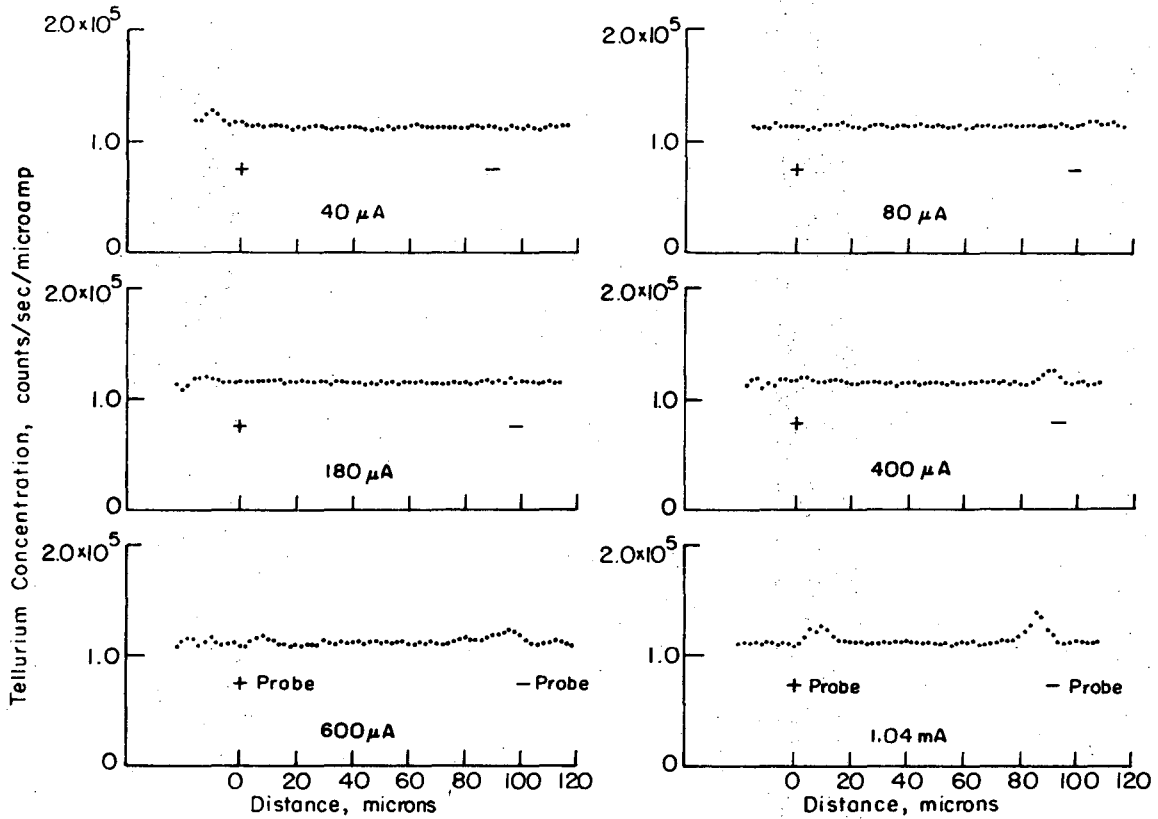
Fig. 18. Accumulation of tellurium prior to nucleation and growth of a filament. Pulse parameters here are: rise time $t_r = 6$ msec, hold time $t_h = 7$ msec, fall time $t_f = 4$ msec, peak current $I_{max} = 1.5$ mA.
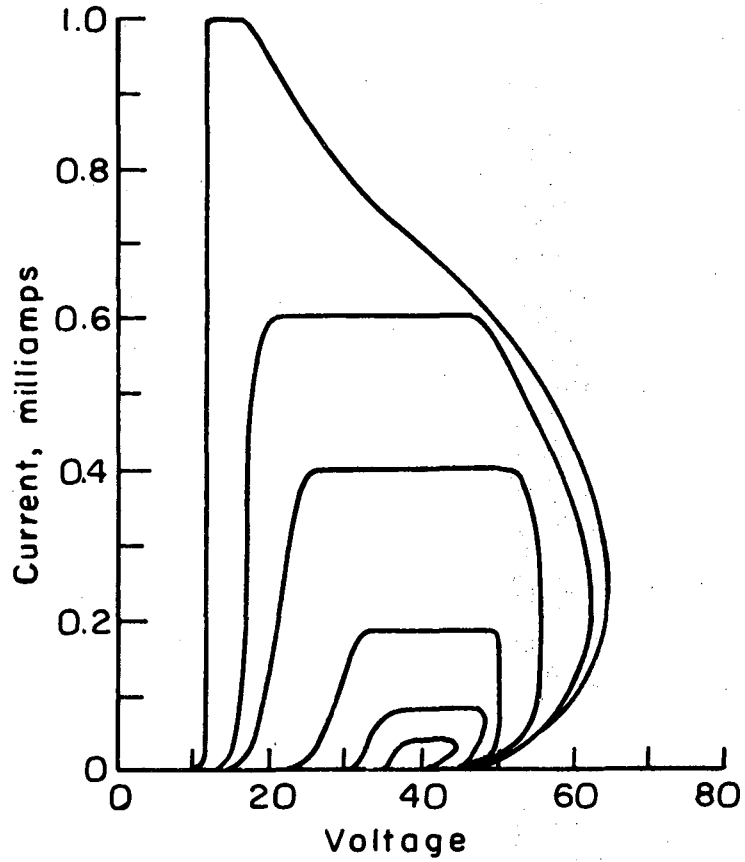
XBL732-5815

XBL736-6310

Fig. 19. Current-voltage curves for the nucleation
experiments.

Fig. 20. Nucleation of the tellurium filament as a function of the
          pulse current level.

are not occurring simultaneously.

D.   Tellurium Concentration Profiles During Growth

To determine the concentration profile in the hillock just beyond the advancing end of the filament, the microprobe traverse was aligned along the axis of the hillock. The low optical magnification available and the curvature of the filaments makes such alignment uncertain. Since this region includes a concentration gradient, "zone leveling" from heating by the electron beam may affect the gradient recorded. Figure 21 shows the profiles of two filaments formed under identical electrical parameters, the traverse of one being up the concentration gradient (of tellurium) and the other down. Since no significant difference can be seen, it is concluded that the concentration gradient is little disturbed by the heating effect of the beam.

1.   Concentration Profiles as a Function of Extent of Growth

A series of partial filaments were prepared, using the same pulse parameters, but varying the extent of completion. A typical partial filament is shown in Fig. 22. The concentration profile in the hillock near the growing end of the filament was found to follow $\exp(-x/\lambda)$, where x is measured from the end of the filament.

Figure 23 plots λ as a function of the extent of growth. This variation shows that the hillock is somewhat depleted axially during growth.

2.   Concentration Profiles as a Function of Segment Length

The segment lengths are small enough compared to the overall filament that they can be considered differential lengths. Thus, the variations of Fig. 23 are not expected to affect the results of this experiment, in which a series of partial filaments are all grown to
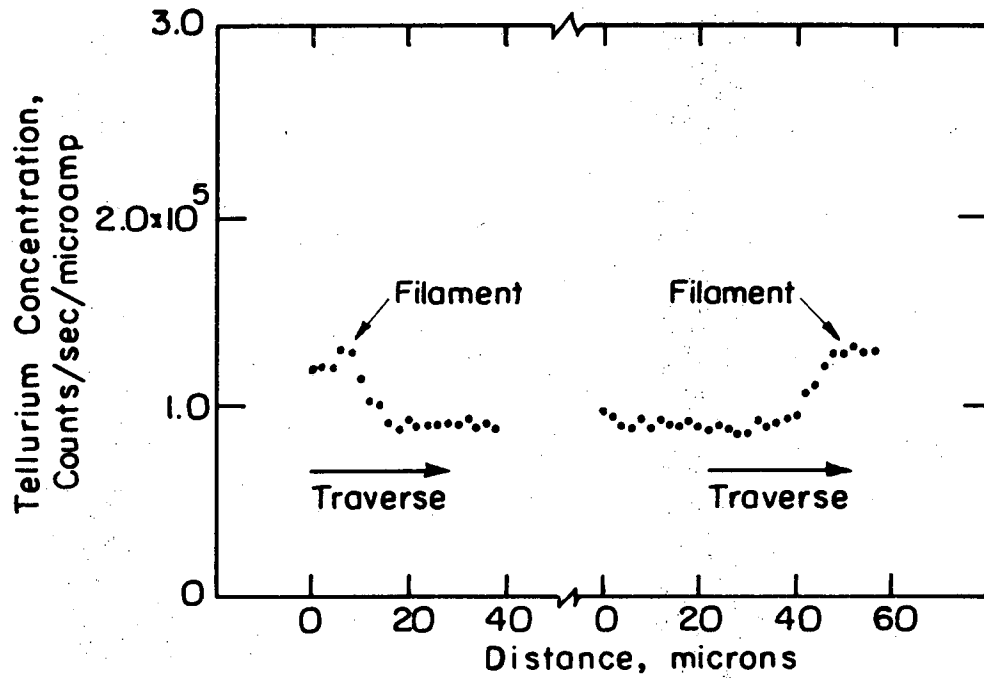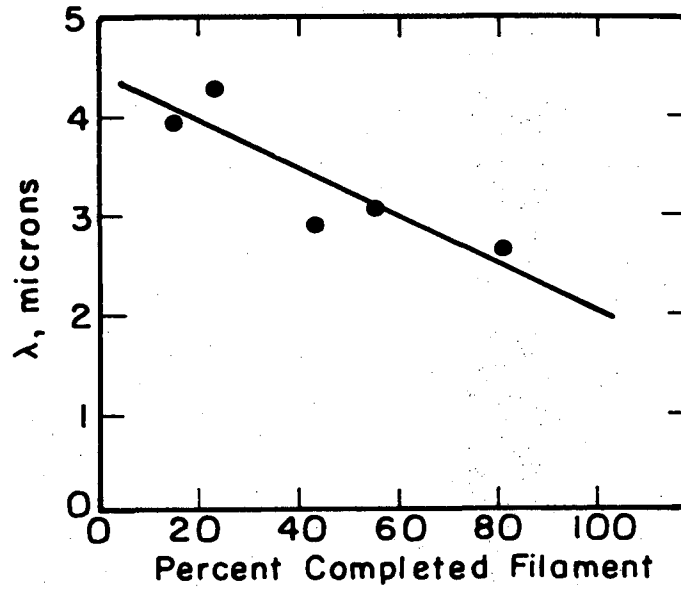
XBL732-5817

Fig. 21. The results of an experimental showing that no
appreciable redistribution of components was
caused by the microprobe beam.
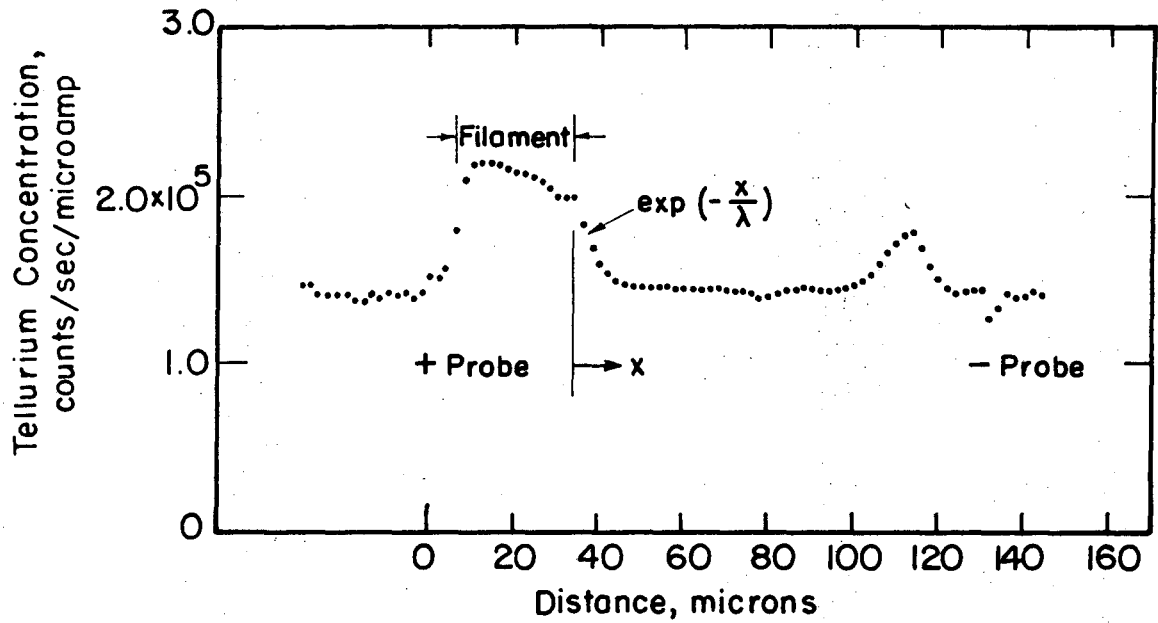
Fig. 22. Axial microprobe traverse of a typical partial filament.

XBL 732-5818

Fig. 23. Concentration gradient parameter λ as a
function of extent of growth.

50% completion, each with different pulse hold times. Figure 24 shows

the variation of the parameter λ under these growth conditions. The

increase in λ suggests that tellurium diffuses from the sides into the

axial region. Since the hillock is being heated by the power dissipation

in the on-states the mobility of tellurium in regions radially more

distant from the axis should increase, approximately as $t_h^{1/2}$, and there-

fore diffuse to the filament tip from further away as the duration of

applied power continues.

E. Composition of Anomolous Growth

The composition of all anomolous growth from the negative probe,

as well as subsurface filaments, has been found to be enriched in

tellurium, although the exact composition cannot be determined by the

microprobe.

F. Discussion

The evidence gathered in this effort show that a crystalline

tellurium path is nucleated at the positive probe contact and grows,

generally as a single crystal, to meet the negative probe or tellurium

crystallites which have formed at the negative probe. The growth

rate, as measured in segmented filaments, is independent of applied

current, linear in time, and approximately independent of extent of

growth. Since the concentration profiles taken from the microprobe

data show no depleted region, we assume that the depleted volume is

large, compared to the volume of filament. The depleted region is

evidently not entirely on the axis of the hillock, since λ of Fig. 24

should decrease with increased hold time if this were true. We can

estimate the volume of matrix required to form a unit length of filament.
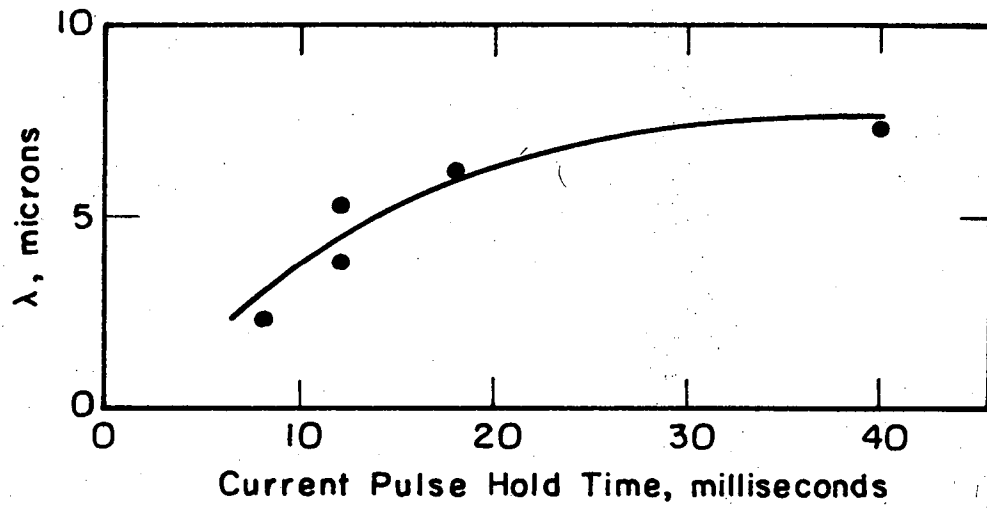
XBL732-5819

Fig. 24. Concentration gradient parameter λ as a function of
current pulse hold time.

For example, a semicircular cylinder of radius ~10μ, depleted uniformly
of 1% of its tellurium concentration, is sufficient to form a filament
2μ wide and 0.2μ thick. A depletion of 1% is too small to detect by
the microprobe analysis. The diameter of such a volume is commensurate
with the width of the hillocks. The fact that the growth rate is constant
is a further indication that the larger component of the tellurium
motion is radial. Axial flow would deplete the hillock axially, and
the growth rate would decrease with time.

IX. CONCLUSIONS

Switching in this composition occurs after the dissipation of sufficient energy to soften the glass. Both the surface distortion and the smoothing of the microprobe data show this has occurred, and the energy dissipated during the peak current level of the pulse should not fail to heat the switched volume to the liquid state.

Filaments formed electrically were found by electron diffraction and microprobe studies to be crystalline tellurium, and often composed of a single crystal joining the two electric contacts. The tellurium atoms drift toward the positive probe under the influence of the applied electric field; consequently, the tellurium must be negatively ionized, an event probably associated with the switching. The motion of tellurium is restricted to a volume extending about 10 microns around the growing end of the filament, and can be associated with the concentrated electric field existing there as a consequence of the geometry. Accumulation of tellurium at the positive probe occurs at current levels greater than 1 mA, although the growth rate of filaments is not enhanced by higher levels. Thus the higher mobility of tellurium expected by heating to higher temperatures electrically must be balanced by a reduction in the field concentration.

In considering the application of the memory state of this material it should be noted that the peripheral equipment requirements are rather severe. Very short filaments could possibly be formed with a single pulse; but for probe spacings in excess of 100 microns, the low duty cycle of pulsed current application is regulated to prevent overheating.

ACKNOWLEDGEMENTS

REFERENCES

1. P. O. Silva, et al. J. of Non-Crystalline Solids $\underline{2}$, 316 (1970).

2. H. J. Stocker, J. Non-Crystalline Solids $\underline{2}$, 371 (1970).

3. D. Shanefield, J. Non-Crystalline Solids $\underline{2}$, 382 (1970).

4. B. K. Ridley, Proceedings of the Physical Society (London) $\underline{82}$, 954 (1963).

5. A. D. Pearson, IBM Journal of Research and Development $\underline{13}$, 510 (1969).

6. F. A. Shunk, Constitution of Binary Alloys (McGraw-Hill, N. Y., 1969) p. 63

7. R. Uttecht, et al., J. Non-Crystalline Solids $\underline{2}$, 358 (1970).

8. I. S. Brammer, M. A. P. Dewey, Specimen Preparation for Electron Microscopy (American Elsevier Publishing Co. Inc., N. Y., 1969).